

Noise and Neuronal Heterogeneity

Michael J. Barber *

Universidade da Madeira, Centro de Ciências Matemáticas, Campus Universitário da Penteada, 9000-390 Funchal, Portugal, michael.barber@arcs.ac.at

Manfred L. Ristig

Institut für Theoretische Physik, Universität zu Köln, D-50937 Köln, Germany, ristig@thp.uni-koeln.de]

Abstract

We consider signal transaction in a simple neuronal model featuring intrinsic noise. The presence of noise limits the precision of neural responses and impacts the quality of neural signal transduction. We assess the signal transduction quality in relation to the level of noise, and show it to be maximized by a non-zero level of noise, analogous to the stochastic resonance effect. The quality enhancement occurs for a finite range of stimuli to a single neuron; we show how to construct networks of neurons that extend the range. The range increases more rapidly with network size when we make use of heterogeneous populations of neurons with a variety of thresholds, rather than homogeneous populations of neurons all with the same threshold. The limited precision of neural responses thus can have a direct effect on the optimal network structure, with diverse functional properties of the constituent neurons supporting an economical information processing strategy that reduces the metabolic costs of handling a broad class of stimuli.

1 Introduction

Neural network models are often constructed of simple units. Typically, model neurons have a particular threshold or bias, and saturate to a fixed value for either strong or weak inputs. Some such models can in fact be derived by systematic approximations of more detailed models such as the Hodgkin-Huxley model (Abbott and Kepler, 1990); many other models are derived from alternative heuristic or phenomenological assumptions. Networks of even the simplest models are well known to be capable of representing complex functions.

*Present address: ARC systems research GmbH, Donau-City-Straße 1, 1220 Vienna, Austria

In this chapter, we investigate the degree to which the simple dynamics of an individual unit limit the inputs that can be processed, and how these limitations can be overcome. To do this, we consider the response of model neurons to a variety of stimuli. The precision of the responses for biological neurons have been shown to be rather limited, typically in the range of a few bits for each action potential or “spike” (Rieke et al., 1997). We mimic this limited precision in the model neurons by including noise in the systems. We focus on intrinsic neuronal noise which has identical statistics for each of the units in the neural network.

Noise is usually viewed as limiting the sensitivity of a system, but nonlinear systems can react to noise in surprising ways. Perhaps the best known of these is the phenomenon known as stochastic resonance (SR), wherein an optimal response to weak or subthreshold signals is observed when a non-zero level of noise is added to the system (Gammaitoni et al., 1998). For example, a noise-free, subthreshold neuronal input can occasionally become suprathreshold when noise is added, allowing some character of the input signal to be detected. SR has been observed and investigated in many systems, ranging from resonant cavities to neural networks to the onset of ice ages (see, e.g., Bezrukov and Vodyanoy, 1997; Gailey et al., 1997; Goychuk and Hänggi, 2000; Jung and Shuai, 2001; Moss and Pei, 1995; Schmid et al., 2001; Wenning and Obermayer, 2003; Wiesenfeld and Moss, 1995).

Collins et al. (1995b) showed, in a summing network of identical Fitzhugh-Nagumo model neurons, that an emergent property of SR in multi-component systems is that the enhancement of the response becomes independent of the power of the noise. This allows networks of elements with finite precision to take advantage of SR for diverse inputs. To build upon the findings of Collins *et al.*, we consider networks of simpler model neurons, but these are allowed to have different dynamics. In particular, we examine noisy McCulloch-Pitts (McP) neurons (Hertz et al., 1991) with a distribution of thresholds. We construct heterogeneous networks that perform better than a homogeneous network with the same number of noisy McP neurons and similar network architecture.

2 Neural Network Model

To investigate the effect of noise on signal transduction in networks of thresholding units, we consider a network of noisy McCulloch-Pitts (McP) neurons. The McP neuron is perhaps the simplest neural model, being only a simple thresholding unit. When the total input to a neuron (signal plus noise) exceeds its threshold, the neuron activates, firing an action potential or “spike.” Formally, the activation state a_i of neuron i in response to some stimulus S can be expressed as

$$a_i(S) = u(S - S_0) \quad , \quad (1)$$

where S_0 is the neuron’s threshold and u is the Heaviside step function, defined as

$$u(x) = \begin{cases} 1 & x > 0 \\ 0 & \text{otherwise} \end{cases} \quad . \quad (2)$$

We model the limited precision of neurons by including noise as an intrinsic¹ feature of the neurons, so that eq. (1) becomes

$$a_i(S) = u(S - S_0 + \eta) \quad , \quad (3)$$

where η is zero-mean, i.i.d. (independent, identically distributed) Gaussian noise with variance σ^2 . We assume the noise distributions to be identical for all the McP neurons.

The network architecture is simple: an input layer of N noisy McP neurons is connected to a single linear output neuron. Each synaptic weight is of identical and unitary strength, so the output neuron calculates the sum of the N input neuron activation states as its response $R_N(S)$:

$$R_N(S) = \sum_{i=1}^N a_i(S) \quad . \quad (4)$$

Each input unit is presented the same analog signal, but with a different realization of the intrinsic neuronal noise.

An important special case is when there is just a single input neuron ($N = 1$). Since the output neuron is a summing unit, its response is just the response of the single input neuron, i.e., $R_N(S) = a_1(S)$. In this chapter, we will use “single neuron” synonymously with “network having only a single input neuron.”

3 Network Response

In this section, we consider the response R_N of the network. Due to the specific choices of neural model and network architecture made in section 2, the resulting neural networks are quite tractable mathematically. A great deal of formal manipulation is thus possible, including exact calculations of the expectation value and variance of the network response.

We initially focus on homogeneous networks with identical input neurons, including the special case of a single input neuron. The stimuli can be chosen without loss of generality so that $S_0 = 0$. The results for $S_0 \neq 0$ can be recovered by a straightforward translation along the S -axis.

The behavior for the standard, noise-free McP neurons is trivial, with all input neurons synchronously firing or remaining quiescent. However, considerably more interesting behavior is possible for noisy McP neurons: subthreshold signals have some chance of causing a neuron to fire, while suprathreshold signals have some chance of failing to cause the neuron to fire.

For a network with N input neurons with the network architecture discussed above section 2, the response R_N of the output neuron is just the number of input neurons that fire. The probability $p(S; \sigma^2)$ of any neuron firing is

$$p(S; \sigma^2) = \frac{1}{\sqrt{2\pi\sigma^2}} \int_{-S}^{\infty} \exp\left(-\frac{x^2}{2\sigma^2}\right) dx \quad , \quad (5)$$

¹Although we conceptually take the noise as intrinsic to the neuron, the model we use is formally equivalent to a noise-free neuron subjected to a noisy stimulus.

while the probability $q(S; \sigma^2)$ for the neuron to remain quiescent is

$$q(S; \sigma^2) = \frac{1}{\sqrt{2\pi\sigma^2}} \int_{-\infty}^{-S} \exp\left(-\frac{x^2}{2\sigma^2}\right) dx . \quad (6)$$

Combining eqs. (5) and (6) gives $q(S; \sigma^2) + p(S; \sigma^2) = 1$, as expected.

Given eqs. (5) and (6), the expectation value $\langle R \rangle(S; \sigma^2)$ and variance $\sigma_R^2(S; \sigma^2)$ when $N = 1$ are

$$\langle R \rangle(S; \sigma^2) = p(S; \sigma^2) \quad (7)$$

$$\sigma_R^2(S; \sigma^2) = p(S; \sigma^2) q(S; \sigma^2) . \quad (8)$$

Since the noise is independent, the probability of different input neurons firing is also independent and the expected value and variance of the output neuron activation are seen to be

$$\langle R_N \rangle(S; \sigma^2) = N p(S; \sigma^2) \quad (9)$$

$$\sigma_{R_N}^2(S; \sigma^2) = N p(S; \sigma^2) q(S; \sigma^2) . \quad (10)$$

The dependence of $\langle R \rangle(S; \sigma^2)$ and $\sigma_R^2(S; \sigma^2)$ on the stimulus S and the noise variance σ^2 is shown in fig. 1.

4 Decoding the Network Output

In this section, we explore the ability of the neural circuit to serve as a signal transducer. We identify limits on the signal transduction capability by decoding the state of the output neuron to reproduce the input stimulus. Near the threshold value S_0 , this gives rise to linear decoding rules. The basic approach is similar to the “reverse reconstruction” using linear filtering that has been applied with great effect to the analysis of a number of biological systems (see, e.g., Bialek and Rieke, 1992; Bialek et al., 1991; Prank et al., 2000; Rieke et al., 1997; Theunissen et al., 1996).

We expand the expected output R_N to first order near the threshold (i.e., $S \rightarrow 0$), giving

$$\langle R_N \rangle(S; \sigma^2) = \frac{N}{2} + \frac{N}{\sqrt{2\pi\sigma^2}} S + O(S^2) . \quad (11)$$

An example of the linear approximation is shown in fig. 2.

Dropping the higher order terms and inverting eq. (11) gives a linear decoding rule of the form

$$\hat{S}_N = \sqrt{2\pi\sigma^2} \left(\frac{R_N}{N} - \frac{1}{2} \right) , \quad (12)$$

where \hat{S}_N is the estimate of the input stimulus. Combining eqs. (9) and (12), we can show that

$$\langle \hat{S}_N \rangle(S; \sigma^2) = \sqrt{2\pi\sigma^2} \left(p(S; \sigma^2) - \frac{1}{2} \right) . \quad (13)$$

The expected value of \hat{S}_N is thus seen to be independent of N ; for notational simplicity, we drop the subscript and write $\langle \hat{S} \rangle$. Examples of $\langle \hat{S} \rangle$ are shown in fig. 3 for several values of the variance σ^2 . Note that, as the noise variance increases, the expected value of the estimated stimulus closely matches the actual stimulus over a broader range.

We must also consider the uncertainty of the value decoded from the network response. This leads to a total decoding error $\Delta \hat{S}_N$ with the form

$$\begin{aligned} \Delta \hat{S}_N^2(S; \sigma^2) &= \left\langle (\hat{S}_N - S)^2 \right\rangle \\ &= \varepsilon^2(S; \sigma^2) + \sigma_{\hat{S}_N}^2(S; \sigma^2) , \end{aligned} \quad (14)$$

where

$$\varepsilon(S; \sigma^2) = \langle \hat{S} \rangle(S; \sigma^2) - S \quad (15)$$

$$\begin{aligned} \sigma_{\hat{S}_N}^2(S; \sigma^2) &= \left\langle (\hat{S}_N - \langle \hat{S} \rangle(S; \sigma^2))^2 \right\rangle \\ &= \frac{2\pi\sigma^2}{N} p(S; \sigma^2) q(S; \sigma^2) . \end{aligned} \quad (16)$$

The expected difference $\varepsilon(S; \sigma^2)$ and the decoding variance $\sigma_{\hat{S}_N}^2(S; \sigma^2)$ are shown in figs. 4.

5 The Role of Noise

The noisy nature of the neurons has a striking and counter-intuitive effect on the properties of the activation state: increasing noise improves signal transmission, as seen in figs. 3 and 4(a). This effect is analogous to the stochastic resonance effect (Gammaitoni et al., 1998). SR can be informally understood as the noise sometimes driving a nominally sub-threshold signal to cross the threshold and producing a current. Signals close to the threshold will more frequently cross the threshold, giving a stronger response than signals far from the threshold.

There are several properties of the activation probabilities that we can derive from eqs. (5) and (6) and that we will find useful for understanding the role of noise in the neural behavior. First, there is a scaling property with the form

$$p(S; \sigma^2) = p(\alpha S; \alpha^2 \sigma^2) , \quad (17)$$

where $\alpha > 0$. Second, there is a reflection property with the form

$$p(S; \sigma^2) = q(-S; \sigma^2) . \quad (18)$$

As the activation probabilities are at the core of essentially all the equations in this chapter, the scaling and reflection properties will be broadly useful to us.

The scaling and reflection properties of the activation probabilities can be used to derive similar properties of the neural responses. The statistics of the neural responses obey the relations

$$\langle R_N \rangle (S; \sigma^2) = 1 - \langle R_N \rangle (-S; \sigma^2) \quad (19)$$

$$\langle R_N \rangle (S; \sigma^2) = \langle R_N \rangle (\alpha S; \alpha^2 \sigma^2) \quad (20)$$

$$\sigma_{R_N}^2 (S; \sigma^2) = \sigma_{R_N}^2 (-S; \sigma^2) \quad (21)$$

$$\sigma_{R_N}^2 (S; \sigma^2) = \sigma_{R_N}^2 (\alpha S; \alpha^2 \sigma^2) , \quad (22)$$

where $\alpha > 0$. Important corollaries of these relations are that $\langle R_N \rangle (S; \sigma^2) = \langle R_N \rangle (-1; (\sigma/V)^2)$ for all $V < 0$, $\langle R_N \rangle (S; \sigma^2) = \langle R_N \rangle (1; (\sigma/V)^2)$ for all $V > 0$, and $\sigma_{R_N}^2 (S; \sigma^2) = \sigma_{R_N}^2 (1; (\sigma/V)^2)$ for all $V \neq 0$. It is thus necessary to consider only one subthreshold stimulus and one suprathreshold stimulus in order to understand the impact of noise on the neural responses; see fig. 5.

Similarly, properties of the statistics for the estimated input \hat{S} can be derived, giving

$$\langle \hat{S} \rangle (-S; \sigma^2) = -\langle \hat{S} \rangle (S; \sigma^2) \quad (23)$$

$$\langle \hat{S} \rangle (\alpha S; \alpha^2 \sigma^2) = \alpha \langle \hat{S} \rangle (S; \sigma^2) \quad (24)$$

$$\varepsilon (-S; \sigma^2) = -\varepsilon (S; \sigma^2) \quad (25)$$

$$\varepsilon (\alpha S; \alpha^2 \sigma^2) = \alpha \varepsilon (S; \sigma^2) \quad (26)$$

$$\sigma_{R_N}^2 (-S; \sigma^2) = \sigma_{R_N}^2 (S; \sigma^2) \quad (27)$$

$$\sigma_{R_N}^2 (\alpha S; \alpha^2 \sigma^2) = \alpha^2 \sigma_{R_N}^2 (S; \sigma^2) , \quad (28)$$

where $\alpha > 0$. Eqs. (23) through (26) imply that $\langle \hat{S} \rangle (S; \sigma^2) = S \langle \hat{S} \rangle (1; (\sigma/S)^2)$ and $\varepsilon (S; \sigma^2) = S \varepsilon (1; (\sigma/S)^2)$ for all $S \neq 0$. Again, we can focus on one subthreshold stimulus and one suprathreshold stimulus to understand the impact of noise (see fig. 6) for the behavior in the two cases, and use straightforward transformation to obtain the exact results for other stimuli.

Further, eq. (14) and eqs. (25) through (28) imply $\varepsilon^2 (S; \sigma^2) = S^2 \varepsilon^2 (1; (\sigma/S)^2)$, $\sigma_{R_N}^2 (S; \sigma^2) = S^2 \sigma_{R_N}^2 (1; (\sigma/S)^2)$, and $\Delta \hat{S}_N^2 (S; \sigma^2) = S^2 \Delta \hat{S}_N^2 (1; (\sigma/S)^2)$ for all $S \neq 0$. Thus, the noise dependence of these latter error sources can be understood with a single stimulus; see fig. 7. Note that the total error $\Delta \hat{S}_N^2 (1; (\sigma/S)^2)$ has its minimum for a nonzero value of the noise variance, analogous to the stochastic resonance effect; see fig. 7.

6 Networks of Heterogeneous Neurons

Thus far, we have focused on single neurons and networks of identical neurons. The effect of multiple neurons has generally been simple, either having no effect on— $\langle \hat{S} \rangle$, ε —or just

rescaling— $\langle R_N \rangle$, $\sigma_{R_N}^2$, $\sigma_{\hat{S}_N}^2$ —the single-channel values.

A significant exception to this general trend is found in $\Delta \hat{S}_N^2$. In fig. 8, we show how $\Delta \hat{S}_N^2$ varies with N . The error curve flattens out into a broad range of similar values, so that the presence of noise enhances signal transduction without requiring a precise relation between S and σ^2 seen for smaller values of N . This effect is essentially the “stochastic resonance without tuning” first reported by Collins et al. (1995a).

Informally stated, SR without tuning allows for a wider range of potentials to be accurately decoded from the channel states for any particular value of the noise variance. To make this notion of “wider range” precise, we again focus our attention on the expected response of the neurons (see fig. 2). The expected neural response $\langle R_N \rangle$ saturates to zero or one when S is far from the neuronal threshold. The width W of the intermediate range can be defined, for example, by taking the boundaries of this range to be the points where the first order approximation reaches the saturation values of zero and one. The width in this case becomes $W = \sqrt{2\pi\sigma^2}$.

Other definitions for the response width are, of course, possible, but we still should observe that the width is proportional to σ , since the activation probability depends only on the ratio of S and σ (eq. (5)). The same width is found for multiple identical input neurons, because the output neuron response is proportional to the single neurons response, without broadening the curve in fig. 2.

The response width can thus be increased by increasing the noise variance σ^2 . As seen in figs. 7 and 8, such an increase ultimately leads to a growth in the decoding error $\Delta \hat{S}_N^2$. In the asymptotic limit as σ^2 becomes large, $\Delta \hat{S}_N^2$ is dominated by $\sigma_{\hat{S}_N}^2$ and we have the asymptotic behavior

$$\Delta \hat{S}_N^2(S; \sigma^2) = O\left(\frac{\sigma^2}{N}\right), \quad (29)$$

based on eq. (16). The growth in $\Delta \hat{S}_N^2$ with increasing σ^2 thus can be overcome by further increasing the number of neurons in the input layer. Therefore, the response width W is effectively constrained by the number of neurons N , with $W = O(\sqrt{N})$ for large N .

An arbitrary response width can be produced by assembling enough neurons. However, this approach is inefficient, and greater width increases can be achieved with the same number of neurons. Consider instead dividing up the total width into M subranges. These subranges can each be independently covered by a subpopulation of N neurons; all neurons within a subpopulation are identical to one another, while neurons from different subpopulations differ only in their thresholds. The width of each subrange is $O(\sqrt{N})$, but the total width is $O(M\sqrt{N})$. Thus, the total response width can increase more rapidly as additional subpopulations of neurons are added. Conceptually, multiple thresholds are a way to provide a wide range of accurate responses, with multiple neurons in each subpopulation providing independence from any need to “tune” the noise variance to a particular value.

To describe the behavior of channels with different thresholds, much of the preceding analysis can be directly applied by translating the functions along the potential axis to obtain the desired threshold. However, system behavior was previously explored near the threshold

value, but heterogeneous populations of neurons have multiple thresholds. Nonetheless, we can produce a comparable system by simply assessing system behavior near the center of the total response width.

To facilitate a clean comparison, we set the thresholds in the heterogeneous populations so that a linear decoding rule can be readily produced. A simple approach that achieves this is to space the thresholds of the subpopulations by $2W$, with all neurons being otherwise equal. The subpopulations with lower thresholds provide an upward shift in the expected number of active neurons for higher threshold subpopulations, such that the different subpopulations are all approximated to first order by the same line. Thus, the expected total number of active neurons leads to a linear decoding rule by expanding to first order and inverting, as was done earlier for homogeneous populations. Note that this construction requires no additional assumptions about how the neural responses are to be interpreted, nor does it require alterations to the network architecture.

To illustrate the effect of multiple thresholds, we begin by investigating the response of a homogeneous baseline to a stimulus S . The baseline network consists of $M = 1$ populations of $N = 1000$ neurons with $S_0 = 0$ and variance $\sigma^2 = 1$. Using the definition above, the response width is $W = \sqrt{2\pi}$. We then consider two cases, homogeneous and heterogeneous, in each of which we increase the response width by doubling the number of neurons while maintaining similar error expectations for the decoded stimuli.

In the homogeneous case, we have a single population ($M = 1$) with $N = 2000$ neurons. Doubling the number of neurons allows us to double the variance to $\sigma^2 = 2$ with similar expected errors outside the response width. Thus, we observe an extended range, relative to the baseline case, in which we can reconstruct the stimulus from the network output (fig. 9).

In the heterogeneous case, we instead construct two subpopulations ($M = 2$) with $N = 1000$ neurons. We leave the variance unchanged at $\sigma^2 = 1$. One of the subpopulations is modified so that the thresholds lie at $+W/2 = \sqrt{\pi/2}$, while the other is modified so that the thresholds lie at $-W/2 = -\sqrt{\pi/2}$. The resulting neural network has a broad range in which we can reconstruct the stimulus from the network response, markedly greater than the baseline and homogeneous cases (fig. 9).

7 Conclusion

We have constructed networks of heterogeneous McP neurons that outperform similar networks of homogeneous McP neurons. The network architectures are identical, with the only difference being the distribution of neuronal thresholds. The heterogeneous networks are sensitive to a wider range of signals than the homogeneous networks. Such networks are easily implemented, and could serve as simple models of many diverse natural and artificial systems.

The superior scaling properties of heterogeneous neuronal networks can have a profound metabolic impact; large numbers of neurons imply a large energetic investment, in terms of both cellular maintenance and neural activity. The action potentials generated in

neurons can require a significant energetic cost (Laughlin et al., 1998), making the trade-off between reliably coding information and the metabolic costs potentially quite important. Thus, we expect neuronal heterogeneity to be evolutionarily favored, even for quite simple neural circuits.

Although we have used a specific model consisting of thresholding neurons with additive Gaussian noise, we expect that the key result is more widely applicable. The demonstration of the advantage of neuronal heterogeneity largely follows from two factors that are not specific to the model neurons. First, the distance of the input stimulus from the threshold is proportional to the standard deviation of the Gaussian noise, and, second, the total variance of the network response is proportional to the number of input neurons. Ultimately, the heterogeneous thresholds are favorable because the independently distributed noise provides a natural scale for the system.

Acknowledgments

We would like to acknowledge support from the Portuguese Fundação para a Ciência e a Tecnologia under Bolsa de Investigação SFRH/BPD/9417/2002 and Plurianual CCM. The writing of this chapter was supported in part by ARC systems research GmbH.

References

- L. F. Abbott and T. Kepler. Model neurons: From Hodgkin-Huxley to Hopfield. In L. Garrido, editor, *Statistical Mechanics of Neural Networks*, pages 5–18, Berlin, 1990. Springer-Verlag.
- S. M. Bezrukov and I. Vodyanoy. Stochastic resonance in non-dynamical systems without response thresholds. *Nature*, 385(6614):319–21, 1997.
- W. Bialek and F. Rieke. Reliability and information transmission in spiking neurons. *Trends Neurosci.*, 15(11):428–434, 1992.
- W. Bialek, F. Rieke, R. R. de Ruyter van Steveninck, and D. Warland. Reading a neural code. *Science*, 252(5014):1854–1857, 1991.
- J. J. Collins, C. C. Chow, and T. T. Imhoff. Stochastic resonance without tuning. *Nature*, 376:236–238, 1995a.
- J. J. Collins, C. C. Chow, and T. T. Imhoff. Aperiodic stochastic resonance in excitable systems. *Pys. Rev. E*, 52(4):R3321–4, 1995b.
- Paul C. Gailey, Alexander Neiman, James J. Collins, and Frank Moss. Stochastic resonance in ensembles of nondynamical elements: The role of internal noise. *Physical Review Letters*, 79(23):4701–4704, 1997. URL <http://link.aps.org/abstract/PRL/v79/p4701>.

- L. Gammaitoni, P. Hänggi, P. Jung, and F. Marchesoni. Stochastic resonance. *Rev. Mod. Phys.*, 70(1):223–87, 1998.
- I. Goychuk and P. Hänggi. Stochastic resonance in ion channels characterized by information theory. *Phys. Rev. E.*, 61(4):4272–80, 2000.
- J. Hertz, A. Krogh, and R. G. Palmer. *Introduction to the Theory of Neural Computation*. Addison-Wesley Publishing Company, Reading, MA, 1991.
- P. Jung and J. W. Shuai. Optimal sizes of ion channel clusters. *Europhys. Lett.*, 56(1): 29–35, 2001. doi: 10.1209/epl/i2001-00483-y.
- Simon B. Laughlin, Rob R. de Ruyter van Steveninck, and John C. Anderson. The metabolic cost of neural information. *Nat Neurosci*, 1(1):36–41, 1998. doi: 10.1038/236.
- F. Moss and X. Pei. Neurons in parallel. *Nature*, 376:211–2, 1995.
- K. Prank, F. Gabbiani, and G. Brabant. Coding efficiency and information rates in transmembrane signaling. *Biosystems*, 55(1–3):15–22, 2000.
- F. Rieke, D. Warland, R. R. de Ruyter van Steveninck, and W. Bialek. *Spikes: Exploring the Neural Code*. MIT Press, Cambridge, MA, 1997.
- G. Schmid, I. Goychuk, and P. Hänggi. Stochastic resonance as a collective property of ion channel assemblies. *Europhys. Lett.*, 56(1):22–28, 2001. doi: 10.1209/epl/i2001-00482-6.
- F. Theunissen, J. C. Roddey, S. Stufflebeam, H. Clague, and J. P. Miller. Information theoretic analysis of dynamical encoding by four identified primary sensory interneurons in the cricket cercal system. *J. Neurophysiol.*, 75(4):1345–64, 1996.
- G. Wenning and K. Obermayer. Activity driven adaptive stochastic resonance. *Physical Review Letters*, 90(12):120602, 2003. URL <http://link.aps.org/abstract/PRL/v90/e120602>.
- K. Wiesenfeld and F. Moss. Stochastic resonance and the benefits of noise: From ice ages to crayfish and SQUIDS. *Nature*, 373:33–36, 1995.

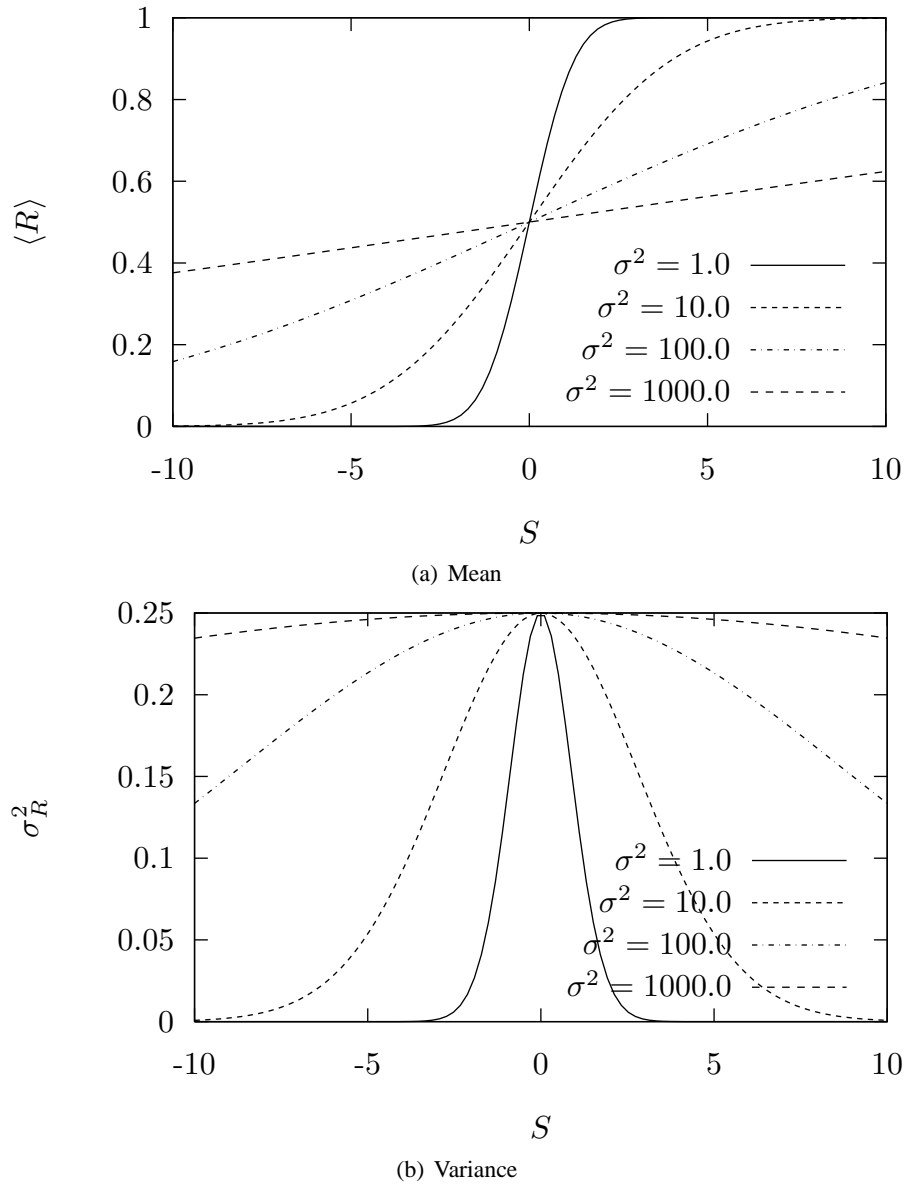


Figure 1: Statistics of single neuron activation. As the noise variance σ^2 increases, (a) the mean activation state $\langle R \rangle (S; \sigma^2)$ takes longer to saturate to the extreme values, while (b) the variance $\sigma_R^2 (S; \sigma^2)$ of the activation state increases with the noise variance.

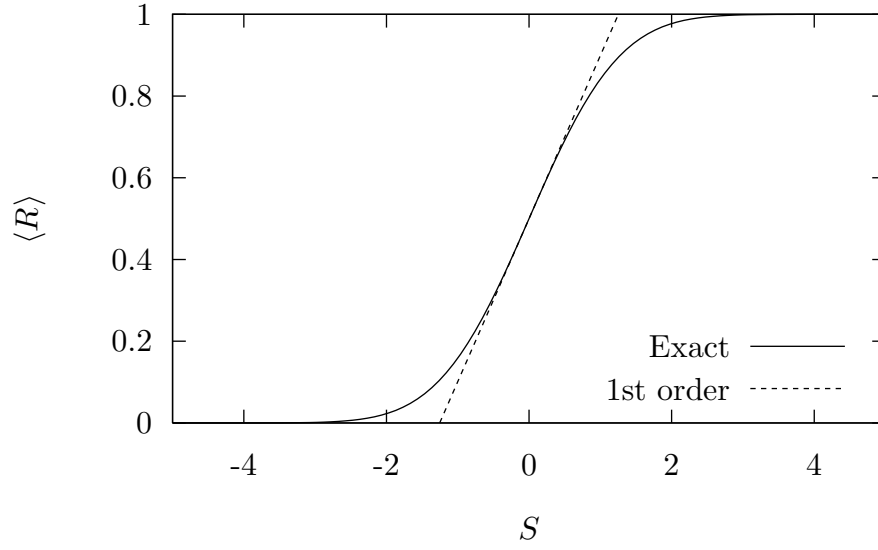


Figure 2: First order approximation of the expected activation of a single neuron. Near the threshold ($S_0 = 0$), the expected activation is nearly linear. Further from the threshold, the activation saturates at either zero or one and diverges from the linear approximation. The values shown here are based on noise variance $\sigma^2 = 1$.

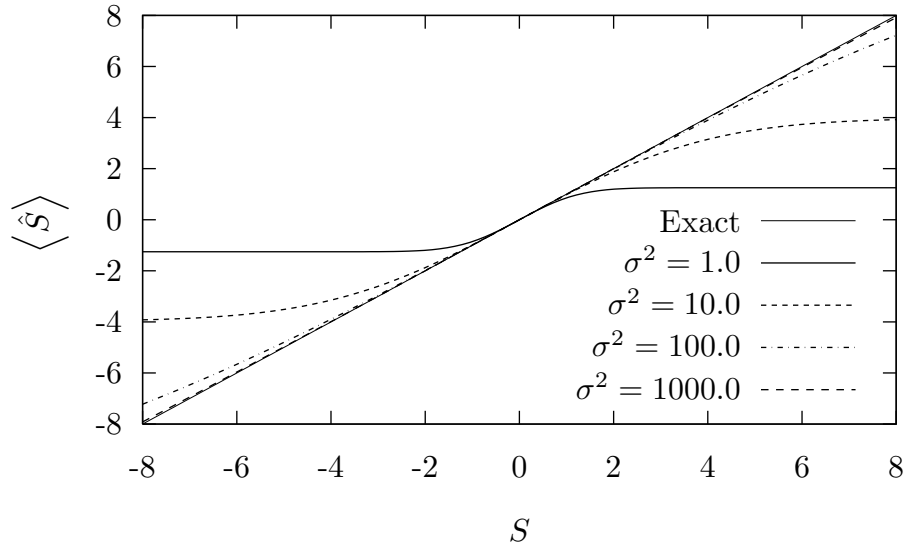


Figure 3: Expectation value of the stimulus decoded from the output of a single neuron. As the noise variance σ^2 increases, the expectation value of the decoded stimulus approximates the true value of the stimulus over an interval of increasing width.

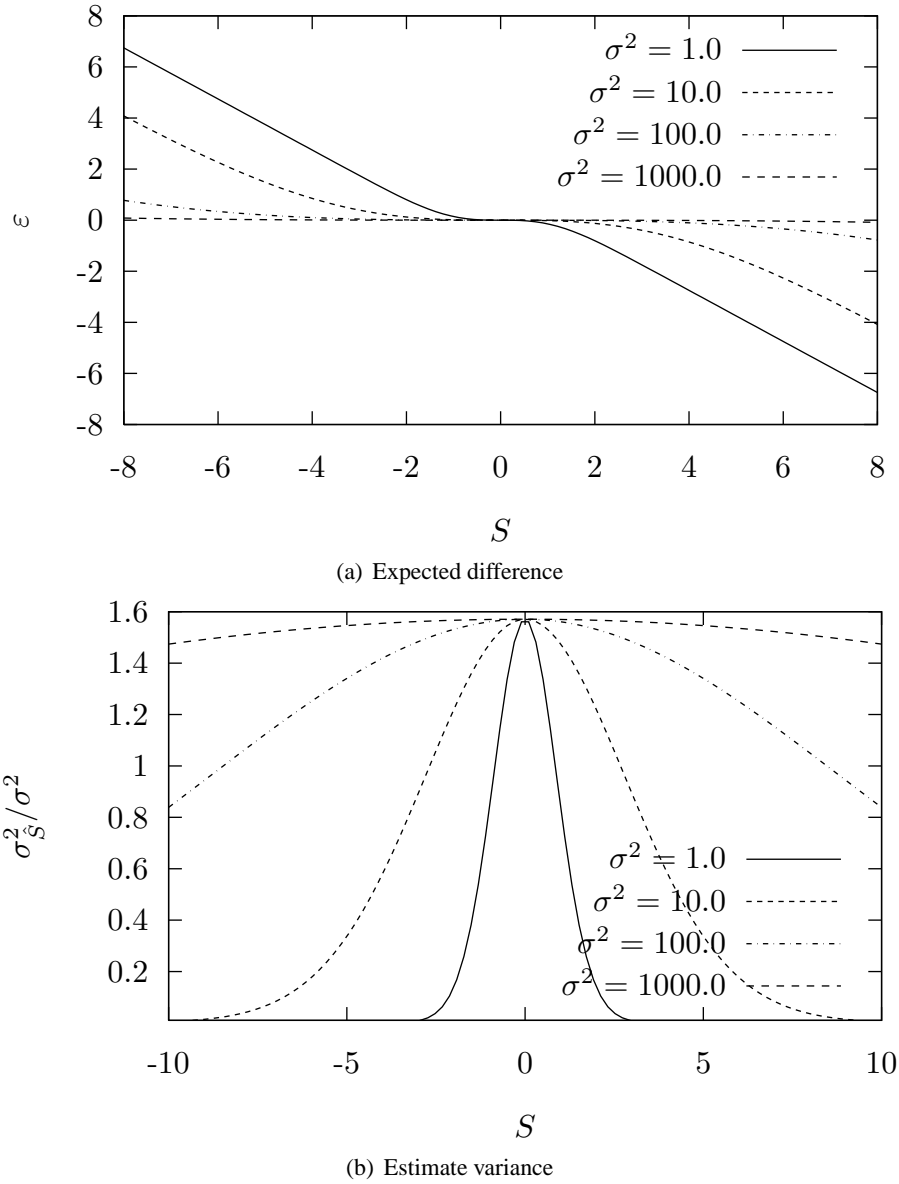
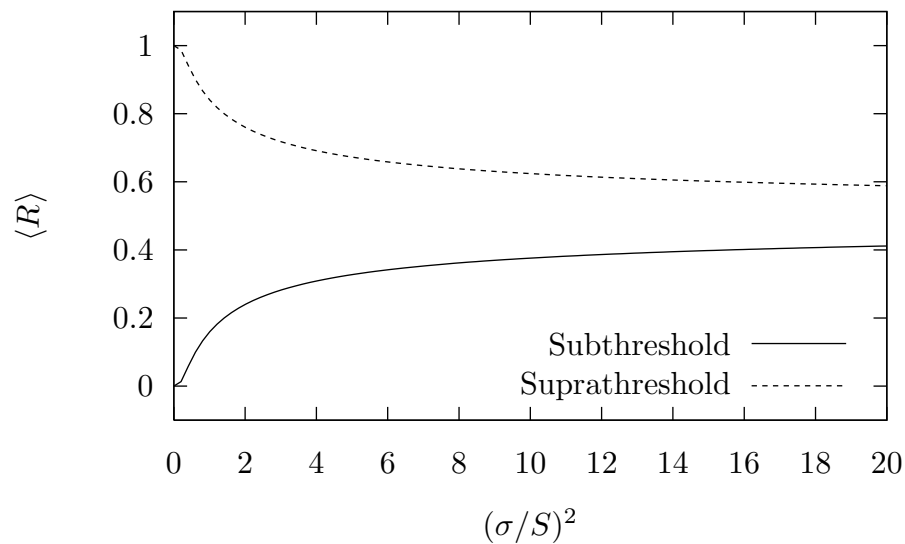
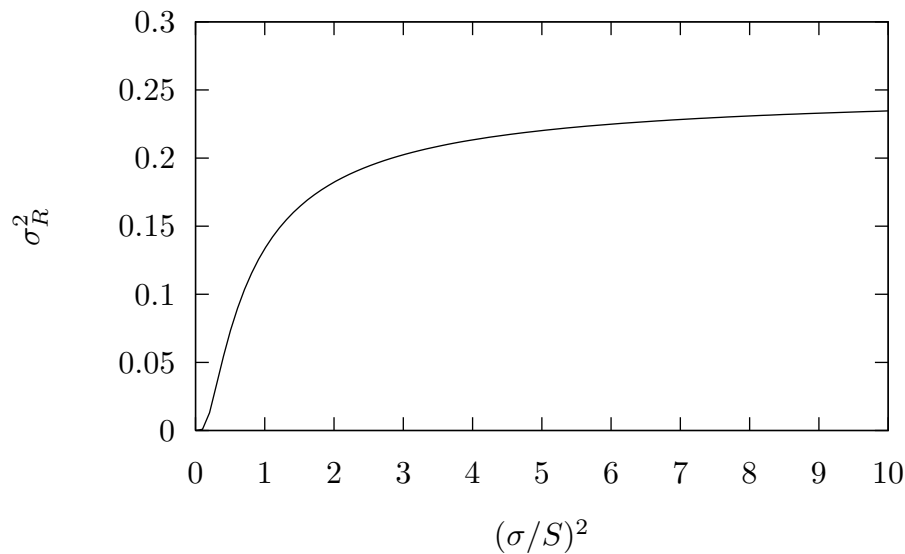


Figure 4: (a) Expected difference between the stimulus and the value decoded from the single-neuron response. The decoded value systematically diverges from the true value as the input gets farther from the threshold value at zero. (b) Variance of the decoded stimulus values. Again, the variances shown here are based on decoding the single-neuron response. The variance of the neuronal noise has been used to scale the variances of the estimates into a uniform range.

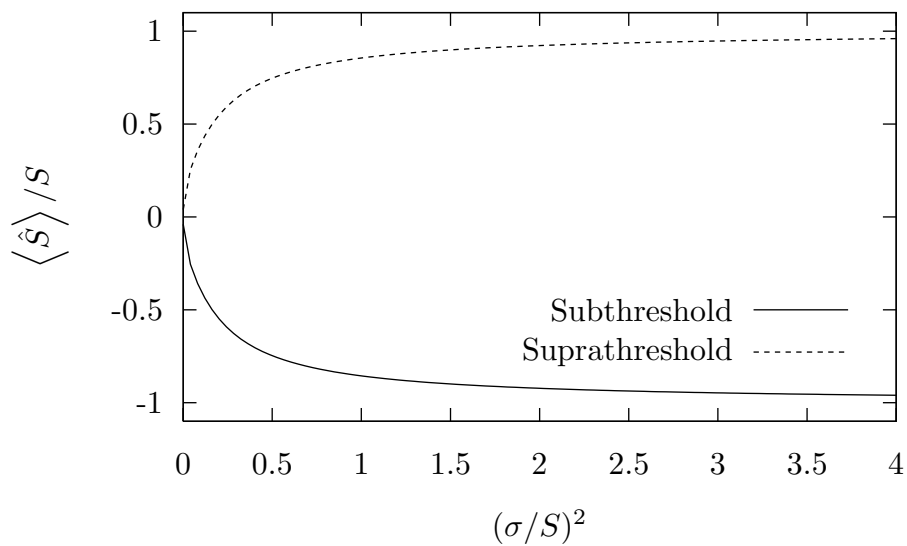


(a) Mean

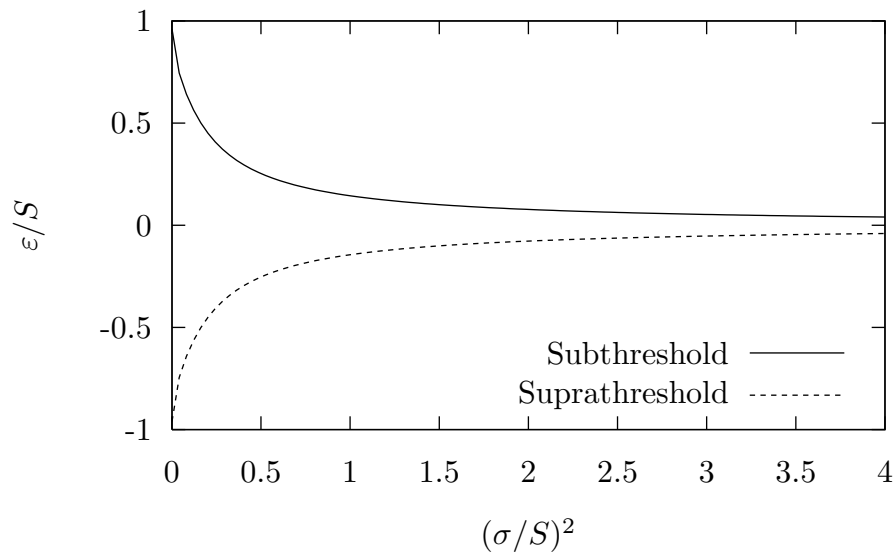


(b) Variance

Figure 5: (a) Noise dependence of single-neuron mean activation. For large values of $(\sigma/S)^2$, the expected activation state asymptotically approaches $1/2$. (b) Noise dependence of single-neuron activation variance. For large values of $(\sigma/V)^2$, the variance asymptotically approaches $1/4$.



(a) Estimated stimulus



(b) Expected difference

Figure 6: (a) Noise dependence of the single-neurons estimated stimulus. For large values of $(\sigma/S)^2$, the estimates for the subthreshold and suprathreshold signals asymptotically approach -1 and $+1$, respectively. (b) Noise dependence of the expected difference. For large values of $(\sigma/S)^2$, the expected differences asymptotically approach 0 for both the subthreshold and suprathreshold signals.

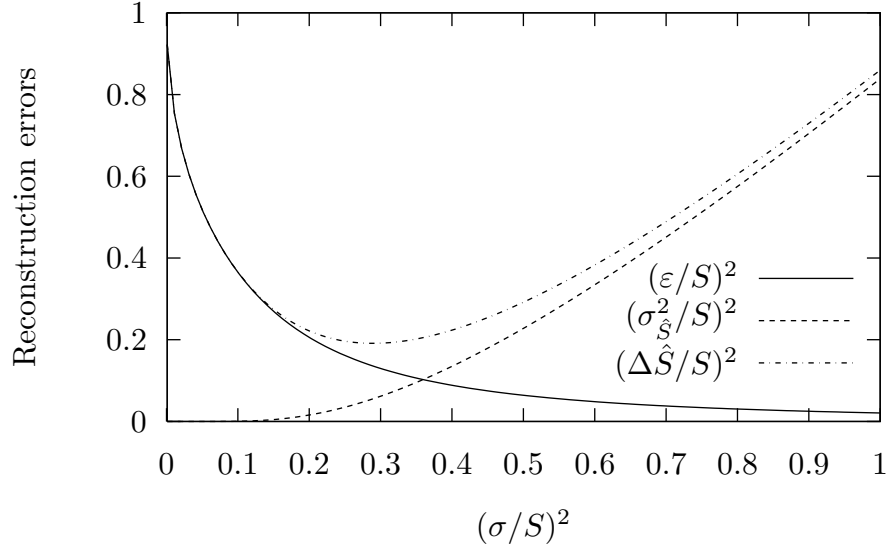


Figure 7: Comparison of decoding error sources. The values shown here are calculated from the response of a single neuron. The minimum in $\Delta\hat{S}^2$ occurs for a nonzero noise variance of the signal, as with stochastic resonance.

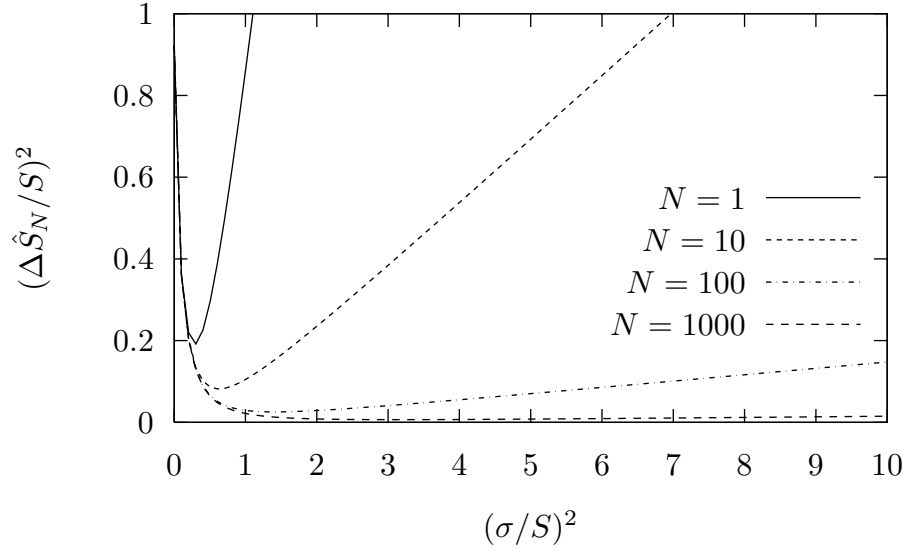
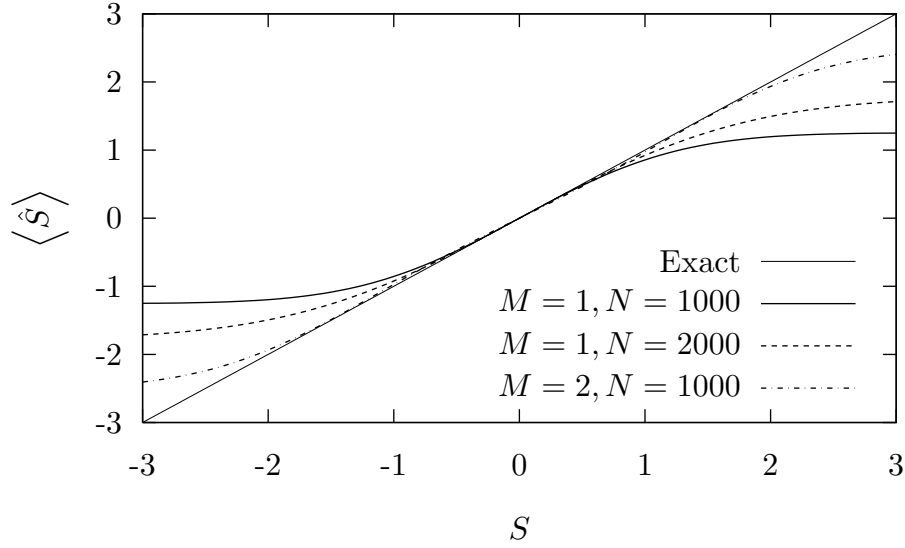
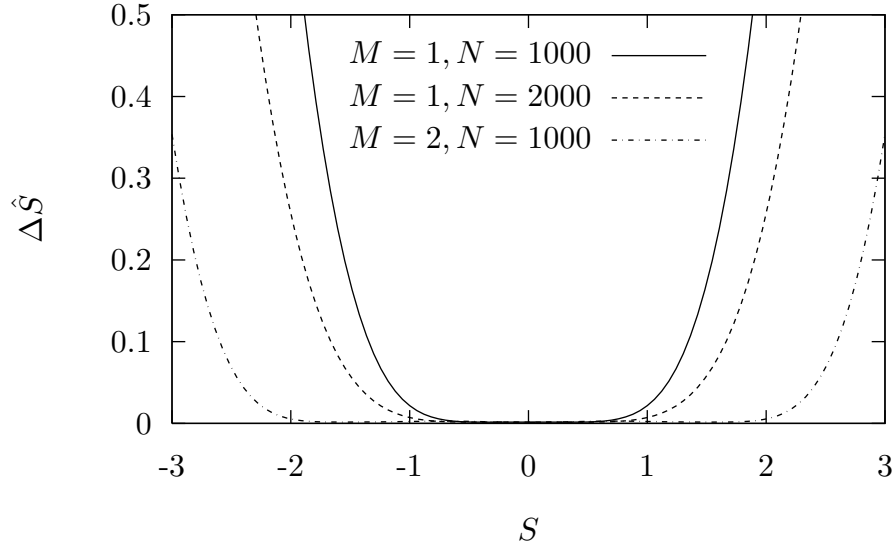


Figure 8: Effect of the number of neurons on the decoding error. As N becomes large, the error curve flattens out, indicating a broad range of noise values that all give similar accuracy in the decoding process.



(a) Decoded stimulus



(b) Decoding error

Figure 9: (a) Expectation value of the decoded output in homogeneous and heterogeneous networks. The response of the heterogeneous neural network ($M = 2, N = 1000$) can be accurately decoded over a broader range than the responses of the baseline ($M = 1, N = 1000$) and homogeneous ($M = 1, N = 2000$) networks. (b) Total decoding error for homogeneous and heterogeneous networks. The heterogeneous neural network has a broader basin of low error values than the baseline and homogeneous networks.